Zhou *et al. Journal of Translational Medicine* (2025) 23:217
https://doi.org/10.1186/s12967-025-06214-x

Journal of Translational Medicine

RESEARCH **Open Access**

# Monocytic myeloid-derived suppressor cells contribute to the exacerbation of bone destruction in periodontitis

Zhaocai Zhou[1†], Chi Zhan[1†], Wenchuan Li[2†], Wenji Luo[1], Yufeng Liu[2], Feng He[2], Yaguang Tian[3*], Zhengmei Lin[1*] and Zhi Song[1*]

## Abstract

**Background** Periodontitis (PD) is a chronic infectious and inflammatory disease characterized by alveolar bone loss. The distinctive activity of immune cells critically exacerbates bone resorption in PD. Myeloid-derived suppressor cells (MDSCs) are known to contribute to various chronic inflammatory conditions, but their role in the pathogenesis and progression of PD remains poorly understood.

**Methods** We used single-cell transcriptomic analysis with human gingival samples and animal models of experimental periodontitis to examine the role of M-MDSCs in PD. We also explored the therapeutic effect of depleting MDSCs on PD in vivo. Additionally, the mechanisms of long non-coding RNA Neat1 and the pathway of NF-κB-dependent "canonical NLRP3 inflammasome activation" in MDSCs were investigated in PD.

**Results** In this study, we revealed that monocytic (M)-MDSCs were significantly increased in inflamed gingiva of PD patients compared to healthy individuals. Expansion of M-MDSCs was also observed in the mouse model of ligature-induced periodontitis, and depletion of MDSCs in PD mice could ameliorate alveolar bone loss and reduce periodontal inflammation. Mechanistically, we found that long non-coding RNA Neat1 was significantly upregulated in M-MDSCs, which achieved this proinflammatory effect by activating NF-κB signaling in PD. Furthermore, the pathway of NF-κB-dependent "canonical NLRP3 inflammasome activation" was confirmed in the PD mouse model, accompanied by increased secretion of proinflammatory cytokines that drive alveolar bone loss, including IL-1β, IL-6 and TNF-α.

[†]Zhaocai Zhou, Chi Zhan and Wenchuan Li contributed equally to this work.

*Correspondence:
Yaguang Tian
yaguangtian@163.com
Zhengmei Lin
linzhm@mail.sysu.edu.cn
Zhi Song
songzh@mail.sysu.edu.cn

Full list of author information is available at the end of the article

**Conclusions** In conclusion, this study highlights the pivotal proinflammatory role of M-MDSCs in PD and suggests that targeting these cells may represent a novel immunotherapeutic approach. Future research could focus on strategies to specifically target MDSCs for the treatment of periodontitis.

**Keywords** Periodontitis, MDSCs, Inflammation, Neat1, NLRP3

## Introduction

Periodontitis (PD) is a chronic infectious and inflammatory disease affecting the periodontal tissues around the teeth, characterized by periodontal attachment loss, bone resorption, and eventual tooth loss [1]. It ranks as the sixth-most prevalent disease worldwide and is the leading cause of tooth loss in adults [2]. The pathogenesis of periodontitis is primarily driven by the host inflammatory response to bacterial presence, which, in turn, leads to immune cell-mediated self-degradation of the periodontal tissues [3]. While bacteria are essential triggers, it is the persistent inflammatory response that critically exacerbates the disease [3]. Current treatment strategies, such as scaling and root planning, antimicrobials, and novel biomaterials, still face various limitations in terms of clinical efficacy [4]. Therefore, a deeper investigation into the distinctive activities of immune cells in PD is crucial for developing more precise and effective therapeutic approaches for treating PD.

Myeloid-derived suppressor cells (MDSCs) represent a heterogeneous group of immature myeloid cells derived from hematopoietic precursor cells and exhibit T cell immunosuppressive function [5]. MDSCs show a wide range of phenotypes. Classically, MDSCs can be divided into two subpopulations: monocytic (M)-MDSCs and granulocytic (G)-MDSCs, which are morphologically very similar to monocytes and granulocytes, respectively [6]. In mice, a subset marker of MDSCs is defined as $CD11b^{+}Ly6G^{-}Ly6C^{high}$ for M-MDSCs and $CD11b^{+}Ly6G^{+}Ly6C^{-/low}$ for G-MDSCs [7]. MDSCs could contribute to the pathogenesis of chronic inflammatory conditions such as infectious diseases, dysbiosis, autoimmune disorders, or cancer [8]. Recent research on periodontitis and MDSCs has mainly focused on exploring the relationship between periodontitis and systemic diseases. It has been reported that periodontal inflammation facilitates breast cancer metastasis by recruiting MDSCs through pyroptosis-induced interleukin (IL)-1β production and chemokine signaling [9]. Kwack et al. [10] found that in obesity-associated experimental periodontitis, M-MDSCs showed increased accumulation in the spleen and bone marrow. In addition, these cells may serve as osteoclast progenitors and contribute to bone destruction [10]. However, the specific role and contribution of M-MDSCs to the progression of periodontitis remains unclear.

Long non-coding RNAs (LncRNAs) are RNAs of at least 200 base pairs in length with limited protein-coding functions and play crucial roles in various physiological and pathological processes [11]. LncRNA nuclear-enriched abundant transcript 1 (Neat1) is an important regulator of immune responses that contributes to the inflammatory response in inflammatory bowel disease [12]. Neat1 was highly expressed in PD tissues and lipopolysaccharide (LPS)-induced periodontal ligament cells (PDLCs) [13]. The NOD-like receptor family protein 3 (NLRP3) inflammasome plays a critical role in the pathogenesis of various bone and joint diseases, including periodontitis [14]. Zhang et al. reported that Neat1 promotes the activation of NLRP3 inflammasomes in mouse macrophages. This activation stabilizes mature caspase-1, which in turn enhances the production of IL-1β, a key inflammatory mediator [15]. However, the specific roles of Neat1 in M-MDSCs in the context of periodontitis and the association of Neat1 and NLRP3 inflammasome activation in PD are undetermined.

In this study, we hypothesized that M-MDSCs are involved in the pathogenesis and progression of periodontitis. We investigated the distribution of M-MDSCs in human gingival samples through single-cell transcriptomic analysis. On the other hand, we verified the distribution of M-MDSCs both in human gingival samples and in the periodontium of animal models of experimental periodontitis. We also explored the therapeutic effect of depleting MDSCs on PD and further investigated the underlying mechanisms of MDSCs in PD. This may suggest a novel immunotherapeutic approach targeting M-MDSCs for the treatment of periodontitis.

## Methods

### scRNA-seq data processing

Single-cell transcriptomic data of GSE164241 and GSE171213 were downloaded from the Gene Expression Omnibus (GEO; https://www.ncbi.nlm.nih.gov/geo/) database [16, 17]. We selected the samples in the two datasets for this study, including 13 PD cases and 17 of healthy controls (HCs). The scRNA-seq data were aligned and quantified using the Python and Scanpy (v.2.6.0) Python package [18]. To acquire more information about periodontitis, we first generated the object and combined the two datasets. The quality control of the cells was assessed based on three metrics: (1) the number of total UMI count per cell was below 500,000; (2) the number of genes expressed by cells was above 200 and below 10,000; (3) the percentage of mitochondrial genes was below 40%. We then selected 4000 highly variable

genes (HVGs) for downstream analysis using the "scanpy.pp.highly_variable_genes" function. Further integration and batch effects correction for the data were applied using a deep generative model of scVI in the scVI (v.1.2.0) Python package [19]. In addition, potential doublet cells were removed using the Solo model via semi-supervised deep learning in the scVI package [20]. A normalized data matrix was used for downstream analysis.

### Cell clustering and annotation

After data processing, nearest neighbourhood graphs were built using the "sc.pp.neighbours" function, and the community algorithm was applied for clustering using the Leiden function (resolution = 1). The dimensionality of the merged datasets was reduced using Principal Components Analysis (PCA) and Uniform Manifold Approximation and Projection (UMAP), implemented by the "scanpy.tl.umap" function. We identified the 14 major cell types based on well-known marker genes and the marker genes of each cluster by "scanpy.tl.rank_genes_groups" function.

### Identification of M-MDSC cluster

To successfully identify M-MDSC, we extracted monocyte cluster for further analysis. New dimensionality reduction via UMAP, and clustering via Leiden function were generated respectively. According to the marker genes in literature, we finally annotated M-MDSC, monocytes, macrophages, conventional dendritic cell (cDC)1 and cDC2 in monocyte cluster [21, 22].

### Differential gene expression analysis and functional enrichment analysis

To identify differentially expressed genes between PD and healthy individuals in M-MDSCs, M-MDSCs were extracted in monocyte cluster and the function "scanpy.tl.rank_genes_groups" with the Wilcox rank sum test algorithm was used. A volcano plot was plotted by decoupler (v.2.10.0) Python package [23].

With the significance below 0.05, the differentially expressed genes (DEGs) identified in M-MDSCs between PD and HC were used for further functional enrichment analysis. We performed the functional enrichment using the "Over Representation Analysis" in the decoupler package. Hallmark genes for the analysis were selected from MSigDB (https://www.gsea-msigdb.org/gsea/msigdb/), a resource containing a collection of gene sets anno tated to different biological processes. We visualized the most enriched terms and given gene sets by dotplot and Gene Set Enrichment Analysis (GSEA) plot.

### Specimen collection and preparation

Human gingival specimens were collected at the Department of Oral and Maxillofacial Surgery, Hospital of Stomatology, Sun Yat-sen University. The human subject protocol was approved by the Medical Ethics Committee of Hospital of Stomatology, Sun Yat-sen University (KQEC-2022-06), and all participants had informed consent. The gingival specimens from patients with PD were mainly obtained from the extraction of multiple loose teeth that were periodontally hopeless, while the specimens from healthy individuals were collected during the extraction of third molars or gingival resection during surgery for a benign jaw cyst. Throughout the procedure, any excess or unnecessary surrounding gingival tissue was carefully removed. Inclusion criteria for PD included: (1) presenting at least 4 teeth with a probing depth ≥ 4 mm, (2) clinical attachment loss ≥ 3 mm, (3) bleeding on probing index ≥ 2, and (4) severe radiographic bone loss extending to 1/2 of the root. The other inclusion criteria were: (1) patients aged from 20 to 60, (2) no smoking, (3) no systemic diseases, (4) no intake of antibiotics or anti-inflammatory medications in the past 3 months, (5) no periodontal therapy within the last 6 months, (6) no pregnancy or breast feeding, (7) no acute infections or allergies, and no immunosuppressant treatment in the past 3 months.

### Experimental animals

Six- to eight-week-old male C57BL/6 mice were purchased from the Sun Yat-sen University (Guangzhou, China). All experiments were performed with the approval of the Animal Care and Use Committee of Sun Yat-sen University (No. 2024001340). A total of 3 experimental groups are described as follows: (a) Control; (b) PD + vehicle; (c) PD + Gr-1 antibody (Ab). Each group was comprised of 5 mice.

### Ligature-induced periodontitis model

Mice were anaesthetized with 1% Pentobarbital Sodium (RWD, Shenzhen, Guangdong, China). Then, a ligature (5 – 0 silk) was placed around the bilateral maxillary second molars of PD + vehicle group and PD + Gr-1 Ab group for 10 days [24]. Control group did not undergo any treatment. For MDSC depletion, purified anti-mouse Ly6G/Ly6C (Gr-1) antibody (Bio X Cell, clone RB6-8C5) was administered at 200 μg/mouse in PD + Gr-1 Ab group by intraperitoneal injection, three times a week for 4 weeks after ligature removal [25]. PBS was used as vehicle control in other groups. Mice were sacrificed and analyzed 28 days after MDSC depletion.

### Micro-CT

The maxillae from mice were collected and scanned by three-dimensional high-resolution micro-CT (Scano Micro-CT, μCT50, Switzerland). The main parameters were as follows: 70 kV, 114 mA, and 10 μm increments. Three-dimensional microstructural image data were

reconstructed and analyzed by using image analysis software (Mimics Research 21.0, Materialize, Belgium). The cementoenamel junction to the alveolar bone crest (CEJ-ABC) distance was measured at six sites, including mesial, middle, and distal points of both the buccal and palatal sides, and the mean CEJ-ABC distance was then calculated.

#### Histological staining and histopathological evaluation

After harvesting, maxillae fixed in 4% paraformaldehyde (PFA) were decalcified in 0.5 M EDTA for 4 weeks, dehydrated, and embedded in paraffin. Sections were stained with hematoxylin and eosin (H&E) and tartrate-resistant acid phosphatase (TRAP; Jiancheng Technology, Nanjing, China). The distance between CEJ-ABC of the sections stained by H&E was measured to evaluate bone loss. TRAP-positive multinucleated cells (> 3 nuclei) were considered osteoclasts and a sign of bone resorption.

#### Immunofluorescence staining

Tissue specimens were blocked in 10% donkey serum albumin for 30 min at room temperature and then incubated with primary antibody overnight at 4 °C. Fluorescence-conjugated secondary antibodies were then incubated for 1 h at room temperature in the dark. The primary antibodies included CD11b antibody (Abcam Cat# ab133357), HLA-DR antibody (Abcam, Cat# ab92511), CD14 antibody (STARTER Cat# S0B2221). The nuclei were visualized using 4′,6-diamidino-2-phenylindole (DAPI) (Roche, Switzerland) for 10 min. The automated quantitative pathology imaging system (Vectra Polaris, Akoya, USA) was used to obtain fluorescence images.

#### Tissue extraction and single-cell preparations

Mice were sacrificed and periodontal tissues were collected. Gingival tissues were isolated and cut into small fragments, followed by enzymatic digestion with RPMI-1640 medium (Gibco; Thermo Fisher Scientific, USA) containing 4 mg/mL dispase (Roche, Switzerland) and 3 mg/mL collagenase type I (Biofroxx, Einhausen, Germany) at 37 °C for 60 min [26]. The digestion solution was filtered through a 70-μm cell strainer (Biologix Research Company, USA) to obtain a single-cell suspension.

#### Flow cytometry

For surface antigen staining, the cells were first incubated with Fc blocker (BioLegend, San Diego, CA) at 4 °C for 10 min and then with the appropriate antibody in the dark at 4 °C for 30 min. The cells were washed and resuspended with 7AAD viability dye in the dark at 4 °C for 10 min. Cells were rapidly analyzed by flow cytometry after viability dye staining (BioLegend, San Diego, CA, USA). Gating strategies are shown in Figure S3. Data were analyzed using FlowJo V10.8.1 (TreeStar, Ashland, OR, USA).

#### RNA extraction, reverse transcription, and real-time quantitative polymerase chain reaction (RT-qPCR)

Total RNA was extracted from the gingiva with Total RNA Rapid Extraction Kit (GOONIEBIO, Guangzhou, China), and then reverse transcribed into cDNA using PrimeScript RT Master Mix (TaKaRa, Ltd, Osaka, Japan). qPCR was performed to measure gene expression levels in a QuantStudio 5 detection system (Thermo Fisher Scientific, USA) using qPCR SYBR Green Master Mix (Vazyme, Nanjing, China). The primers used in the process are listed in Supplementary Table S1.

#### Western blot analysis

Proteins were extracted from cells and tissues using radioimmunoprecipitation assay (RIPA) buffer (Beyotine, Shanghai, China) for 30 min on ice. The concentration of total protein in RIPA-extracted lysates was measured using a bicinchoninic acid (BCA) protein assay kit (Elabscience, Wuhan, China). Sodium dodecyl sulfate-polyacrylamide gel electrophoresis (SDS-PAGE) was performed to separate the proteins, which were then transferred to a polyvinylidene fluoride membrane (PVDF; Millipore, MA, USA). Skim milk (5%) was used to block the PVDF membranes for one hour at room temperature. The membranes were incubated with the indicated primary antibodies overnight at 4 °C and then incubated with horseradish peroxidase-conjugated secondary antibodies for one hour at room temperature. A chemiluminescence kit (Millipore, MA, USA) was used to detect the target bands. Information of the antibodies used in these experiments was provided in Supplementary Table 3.

#### Enzyme-linked immunosorbent assay (ELISA)

The cytokines in the periodontal tissues were detected with human and mouse IL-1β, IL-6 and TNF-α ELISA kit (Thermo Fisher Scientific, USA) according to the manufacturer's instructions. Briefly, 96-well plates were coated with the capture antibodies overnight at 4℃. After washing and blocking, the diluted supernatants and recombinant cytokine standards were added to the plates and incubated at 37℃ for 2 h. Then, the plates were incubated sequentially with the detection antibodies and streptavidin-HRP, as well as TMB solution and stop solution. The absorbance was measured at 450 nm with wavelength correction set to 570 nm.

#### In vitro MDSC induction and T cell proliferation assay

Bone marrow (BM) cells from experimental PD mice were isolated and cultured for 7 days in complete 1640 medium supplemented with cytokines including

granulocyte-macrophage colony stimulating factor (GM-CSF; 40 ng/ml, Proteintech). Cultures were run in duplicate, and the media and cytokines were refreshed every 3 days. Spleen-derived $CD3^+$ T cells from C57BL/6 mice were labeled with carboxyfluorescein succinimidyl ester (CFSE) (BioLegend, San Diego, CA). CFSE-labeled T cells were co-cultured with isolated MDSCs (including G-MDSCs and M-MDSCs) from BM cells in 96-well plates at a ratio of 1:0, 1:1, and 2:1 for 72 h in medium containing Mouse T-Activator CD3/CD28 (BioLegend, San Diego, CA). CFSE intensity was quantified by flow cytometry.

### Statistics

Quantitative data are expressed as mean ± standard deviation (S.D.). A two-tailed Student's t-test was used for comparisons between two groups. Multigroup comparisons were performed using one-way analysis of variance (ANOVA) followed by the correction of Bonferroni. A *p*-value of less than 0.05 was considered statistically significant. All statistical analyses were performed using the SPSS 25.0 software.

## Results

### scRNA-seq map landscape of periodontal tissues

To investigate the differences in cell populations between PD patients and healthy individuals, we analyzed two published scRNA-seq datasets: GSE164241 and GSE171213 [16, 17]. The datasets contained cell information from 13 PD cases and 17 healthy cases. In total, we obtained 118,969 single cells after standard data processing and quality filtering, including 62,533 cells from HCs and 56,436 cells from PDs. Each sample and the two groups were profiled based on UMAP (Fig. 1A-B). Leiden clustering identified 14 distinct clusters that were annotated based on specific marker genes in the PD and HC groups (Fig. 1C, Figure S1A-B). In particular, the clusters were as follows: (1) B cell cluster, (2) endothelial cell cluster, (3) epithelial cell cluster, (4) erythrocyte cell cluster, (5) fibroblast cluster, (6) granulocyte-derived cell cluster, (7) mast cell cluster, (8) melanocyte cluster, (9) monocyte subset cluster, (10) NK cell cluster, (11) neutrophil subset cluster, (12) plasma cell cluster, (13) T cell cluster, and (14) plasmacytoid dendritic cell (pDC) cluster. The profiles of the expression differences of the representative marker genes in the cell populations were confirmed by statistical quantification to match the biological annotation in the dot plot and UMAP plot (Fig. 1D-E, Figure S1C).

### M-MDSCs are markedly elevated in inflamed periodontal tissues

M-MDSCs share progenitor cells with monocytes, and recent studies classify M-MDSCs as a heterogeneous population [22]. Consequently, further identification and analysis of M-MDSCs in the monocyte subset cluster in scRNA-seq data were investigated. We successfully identified a distinct M-MDSC population in monocytic subset and cell markers of LYZ, CSF3R, CD14, ITGAM, PADI4, PLBD1, SELL, S100A8 and S100A9 were predominantly expressed in M-MDSCs (Fig. 2A and D). Moreover, the cell number of M-MDSCs is significantly higher in PD than in HC in UMAP (Fig. 2B-C). Similarly, M-MDSCs constituted approximately 13% of the monocyte subset in HC. In contrast, the proportion of M-MDSCs in PD patients was 31%, a 2.4-fold increase compared to healthy individuals (Fig. 2E).

To further confirm whether M-MDSCs are increased in periodontitis, we collected human gingival samples from periodontitis patients or healthy individuals. As expected, the gingival tissues of periodontitis patients showed significantly higher levels of inflammatory cell accumulation compared to those without periodontitis (Figure S2A). In addition, RT-qPCR analysis and ELISA also showed that the proinflammatory cytokines IL-1β, IL-6, and tumor necrosis factor-alpha (TNF-α) mRNA expression and protein levels were significantly increased in the gingival tissues of PD compared with the HC group (Figure S2B-G). Notably, we observed that the number of M-MDSCs ($CD11b^+CD14^+HLA\text{-}DR^{low}$) cells was significantly higher in PD than in the healthy group, which was consistent with the results of single-cell analysis above (Fig. 2F). These results suggest that M-MDSCs may infiltrate and expand in the inflamed periodontium.

### Depletion of MDSCs rescues epithelial lesions and alveolar bone loss in PD mice

Previous reports have documented the induction and infiltration of MDSCs in arthritis, as well as the plasticity of M-MDSCs under various pathological conditions related to bone destruction [27]. However, the identity, proinflammatory role, and molecular mechanisms of MDSC subsets in periodontitis remain elusive. We established a periodontitis mouse model and investigated the infiltration of M-MDSCs and G-MDSCs in inflamed gingiva. Flow cytometric analysis revealed that the total proportion of MDSCs ($Gr\text{-}1^+CD11b^+$) in the periodontal tissues of PD mice was 2-fold higher than in healthy mice. Next, we observed that the frequency of M-MDSCs in the gingiva showed an approximately 5-fold increase in PD mice compared to control mice (Fig. 3A-C). However, G-MDSCs show a lower proportion in PD mice compared to controls (Fig. 3D).

To confirm the suppression of T cell proliferation by M-MDSCs in PD, we isolated CD3/CD28-stimulated T cells from bone marrow and co-cultured them with M-MDSCs in vitro. CFSE-labeled CD3 + T cells were cultured with or without M-MDSCs over a period for 3

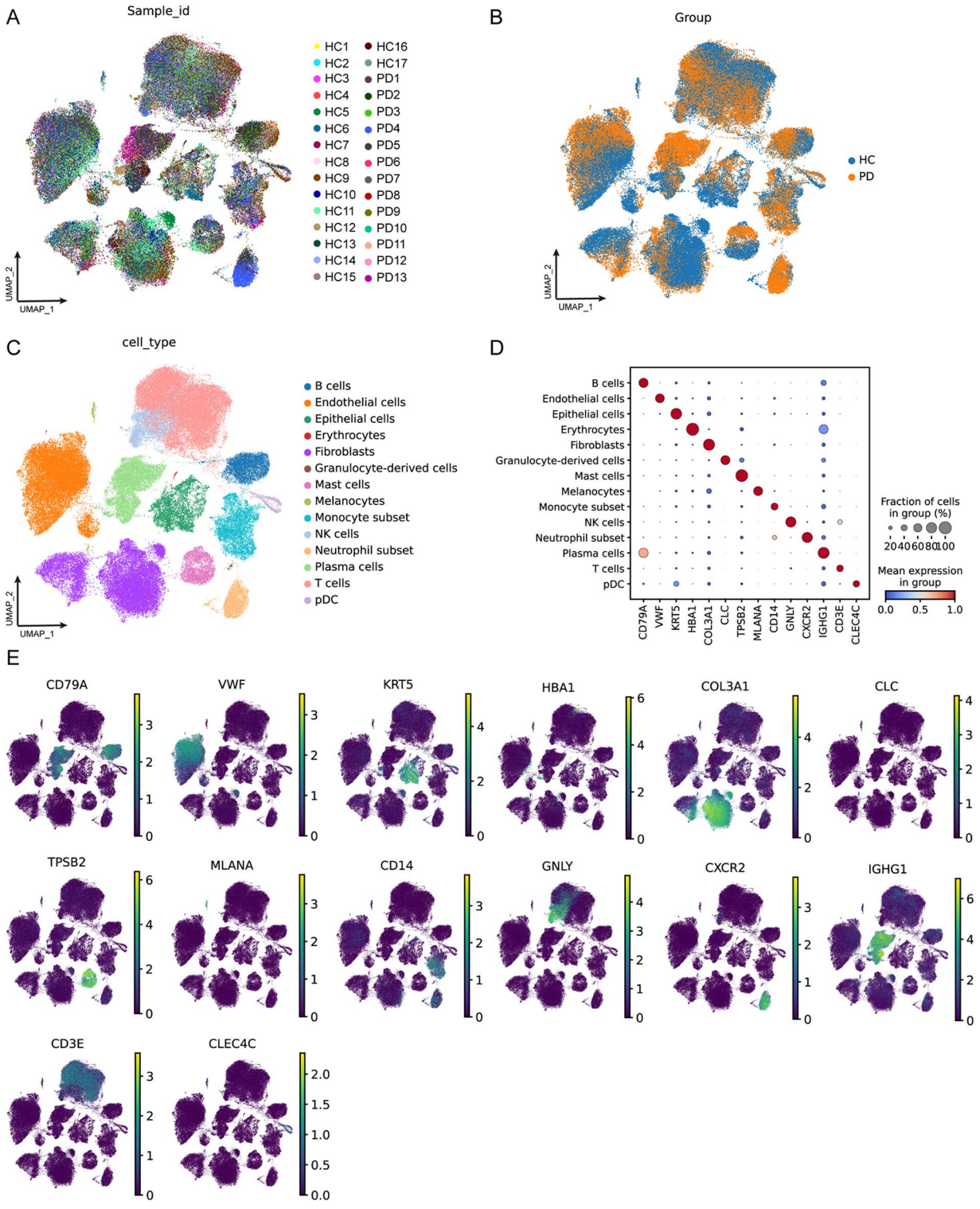


**Fig. 1** Identification of cell annotation from periodontal tissues of healthy controls and periodontitis. (**A**-**B**) Uniform manifold approximation and projection (UMAP) plots showing the distribution of samples (**A**) and disease (**B**). Dots represent single cells. HC, healthy control; PD, periodontitis. (**C**) UMAP plot showing the major cell types. Dots represent single cells, and colors represent different cell populations. NK, natural killer cells; pDC, plasmacytoid dendritic cells. (**D**-**E**) Dot plots and UMAP plots showing the expression of marker genes for clusters in each major cell population, including B cells (CD79A), endothelial cells (VWF), epithelial cells (KRT5), erythrocytes (HBA1), fibroblasts (COL3A1), granulocyte-derived cells (CLC), mast cells (TPSB2), melanocytes (MLANA), monocytes (CD14), NK cells (GNLY), neutrophil subset (CXCR2), plasma cells (IGHG1), T cells (CD3E), and pDC (CLEC4C)

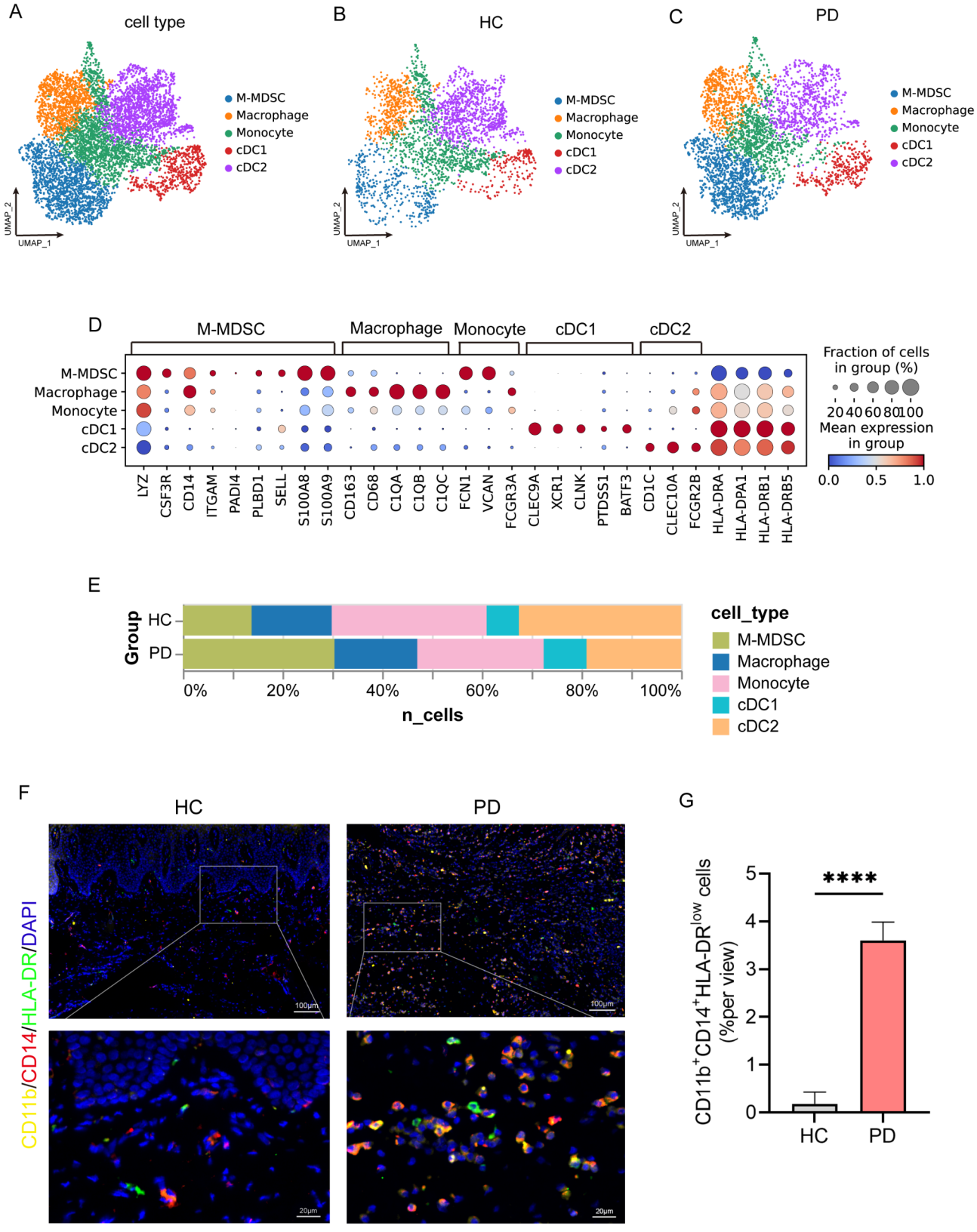


**Fig. 2** (See legend on next page.)

(See figure on previous page.)

**Fig. 2** M-MDSCs were identified and displayed expansion in periodontitis. (**A**-**C**) UMAP plot showing the detailed cell population in monocyte subset of all samples (**A**), HC group (**B**) and PD group (**C**). Dots represent single cells, and colors represent different cell populations. (**D**) Dot plots showing the expression of marker genes for clusters in the monocyte subset, including M-MDSCs (high expression of LYZ, CSF3R, CD14, ITGAM, PADI4, PLBD1, SELL, S100A8, and S100A9; low expression of HLA-DRA, HLA-DRB1, and HLA-DRB5). (**E**) Proportional bar graph representing the cluster frequency of the monocyte subset in the PD and HC groups. In each group, the sum of each cluster percentage is 100%. (**F**) Immunofluorescence (IF) staining of gingival tissues for PD patients and healthy individuals, in which CD11b positive, HLA-DR negative, and CD14 positive represent M-MDSCs. (**G**) Quantification of M-MDSCs in human gingival samples ($n = 3$ per group). The results were presented as means ± S.D. ****$p < 0.0001$ by 2-tailed, unpaired Student's t test. HC, healthy control; PD, periodontitis

days. CD4 + and CD8 + T cells showed baseline proliferation rates of 17.21 and 13.11%, respectively, when cultured alone in stimulation media. When M-MDSCs were added to these cultures at different ratios of (MDSCs: T cells, 1:1/2), CD4 + and CD8 + T cell proliferation decreased significantly, confirming the suppressive function of M-MDSCs (Fig. 3E).

Although MDSCs are best known for their role in suppressing antitumor immunity, recent studies have shown that they also have proinflammatory effects and mediate the progression of inflammation in joint diseases such as gout and rheumatoid arthritis by producing higher levels of IL-1β [28, 29]. To further investigate whether MDSCs play a proinflammatory role in PD, we depleted MDSCs by injecting anti-Gr-1 antibody into PD mice [30]. Anti-Gr-1 Ab or vehicle was administered to experimental mice three times a week for 28 days after ligature removal. This approach resulted in the expected depletion of MDSCs, particularly M-MDSCs in PD (Fig. 3A-D). Subsequently, periodontal tissues were harvested from the experimental mice and subjected to micro-CT and histological analysis. The inflammatory response can lead to alveolar bone resorption and tooth loss [31]. Thus, we investigated the effect of MDSC depletion on alveolar bone. Micro-CT analysis showed that alveolar bone loss was significantly higher in the PD + vehicle group compared to the control group, whereas the alveolar bone loss was reduced by 26.5% in the PD + Gr-1 antibody group compared to the PD + vehicle group (Fig. 4A, D). H&E staining showed that the epithelial layers of the periodontal tissues were thicker in the PD + Gr-1 Ab group compared to the PD + vehicle group. In addition, there were fewer infiltrating inflammatory cells and a less alveolar bone loss in the PD + Gr-1 Ab group Fig. 4B, E). Osteoclasts are involved in bone resorption and inhibit the formation of neonatal alveolar bone formation. TRAP staining revealed significantly fewer osteoclasts in the periodontal tissues of the PD + Gr-1 Ab group than in those of the PD + vehicle group (Fig. 4C, F). These results indicate that depletion of MDSCs rescues alveolar bone loss in PD mice.

### LncRNA Neat1 is significantly up-regulated in M-MDSC cells from PD

We found that MDSCs may promote inflammatory responses in periodontitis. However, the proinflammatory mechanism of M-MDSCs in periodontitis requires further investigation. Therefore, we isolated the M-MDSCs cell cluster and performed a detailed analysis using the previously examined scRNA-seq data. The DEGs between PD patients and healthy individuals of M-MDSCs were identified using a volcano plot. In Fig. 5A, NEAT1, IGKC, NAMPT, MTRNR2L1, CD44, and other genes were upregulated in PD. Gene Ontology (GO) analysis for the DEGs showed that the genes were enriched in pathways associated with inflammation. The top five GO terms were as follows: "TNFA signaling via NFKB", "Interferon gamma response", "Interferon alpha response", "Allograft rejection", and "Inflammatory response" (Fig. 5B). Furthermore, the characteristics of DEGs were investigated in the pathways of TNFA signaling via NFKB and inflammatory response via GSEA were investigated. Upregulated DEGs in PD were significantly enriched in these two inflammatory pathways (Fig. 5C, D).

Notably, Neat1 showed the most statistically significant increase in expression in M-MDSCs from PD patients. Recent studies have shown that Neat1 is upregulated and plays an important role in immunological processes in diabetic nephrology and osteolysis [32, 33]. Therefore, we further explored whether Neat1 could be increased in periodontitis. Since Neat1 has two isoforms, a smaller 3.7-kb isoform (Neat1_1) and a larger 23-kb isoform (Neat1_2), we used two pairs of primers to detect the expression of Neat1 in PD [34]. RT-qPCR analysis showed that both Neat1 and Neat1_2 RNA expression were upregulated in the periodontium, indicating that both Neat1_1 and Neat1_ 2 were dysregulated in patients and mice with PD (Fig. 5E, F; Figure S4A, B). Importantly, Neat1 and Neat1_2 RNA expression was reduced by 36% and 33%, respectively, in the periodontal tissues after depletion of MDSCs in the PD + Gr-1 Ab group compared with those of the PD + vehicle group (Fig. 5E, F). Taken together, these results suggest that Neat1 levels are upregulated in M-MDSCs from PD. Neat1 may be involved in the regulation of inflammation in PD.

### NF-κB-dependent "canonical NLRP3 inflammasome activation" occurred in PD mice

Previous studies have shown that Neat1 promotes the activation of the nuclear factor-kappa-B (NF-κB) signaling, which in turn transcriptionally upregulates the

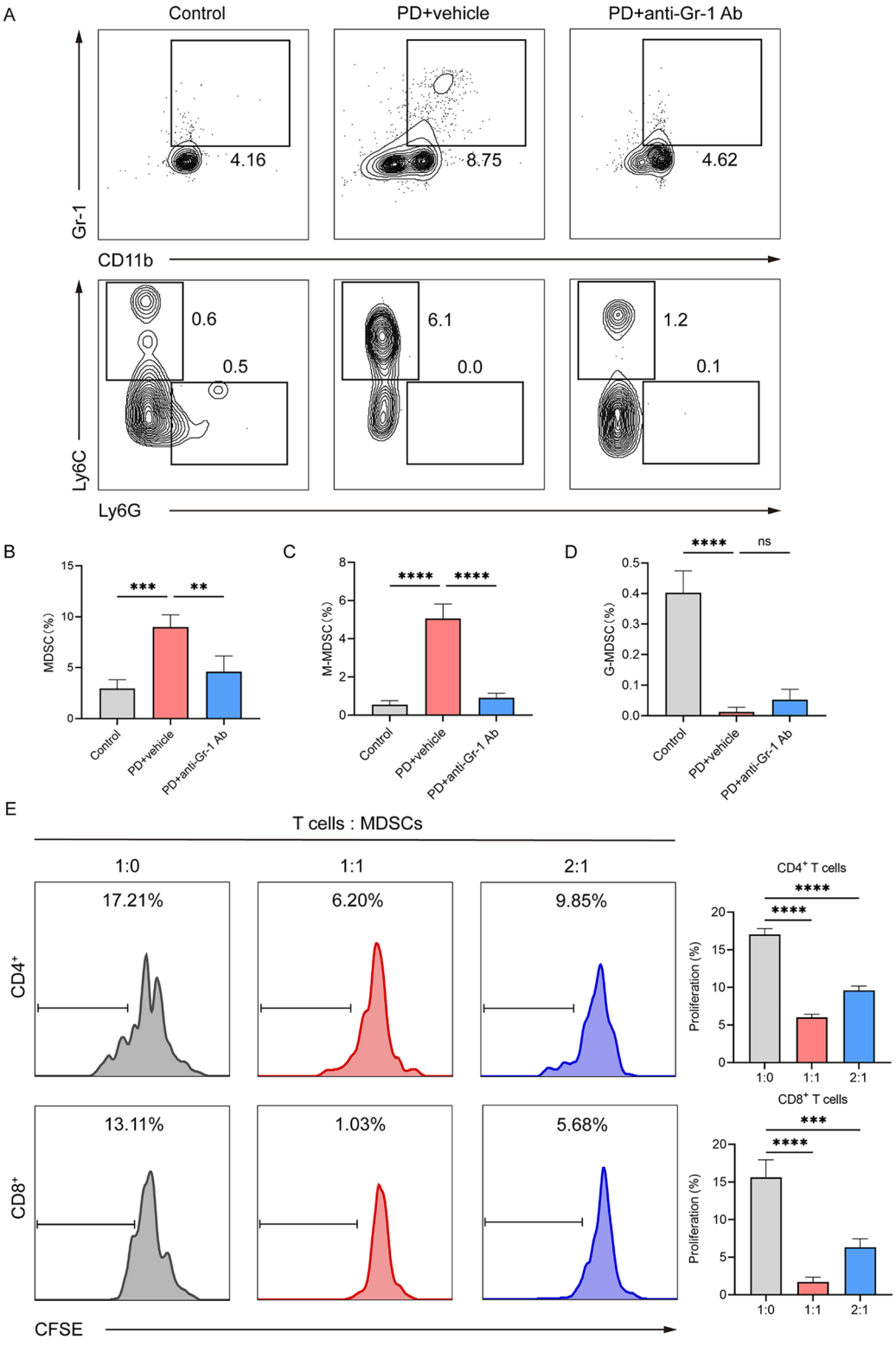


**Fig. 3** The number of M-MDSCs increased in experimental periodontitis and successfully decreased with MDSCs depletion. (**A**) The proportion of M-MDSCs in the CD45$^+$ cell population in the gingiva from control mice, vehicle-treated PD mice and anti-Gr-1 Ab-treated mice on day 28 after ligature removal was analyzed by flow cytometry ($n = 4$ per group). (**B**-**D**) Statistical analysis of flow cytometry data describing the percentage of MDSCs (**B**), M-MDSCs (**C**) and G-MDSCs (**D**) in CD45$^+$ cells from gingiva ($n = 4$ per group). (**E**) Proliferation of CD4$^+$ and CD8$^+$ T cells in the co-culture system was detected by CFSE assay ($n = 3$ per group). The results were presented as means ± S.D. $^{**}p < 0.01$; $^{***}p < 0.001$; $^{****}p < 0.0001$; ns. $p > 0.05$ (one-way ANOVA with the correction of Bonferroni)

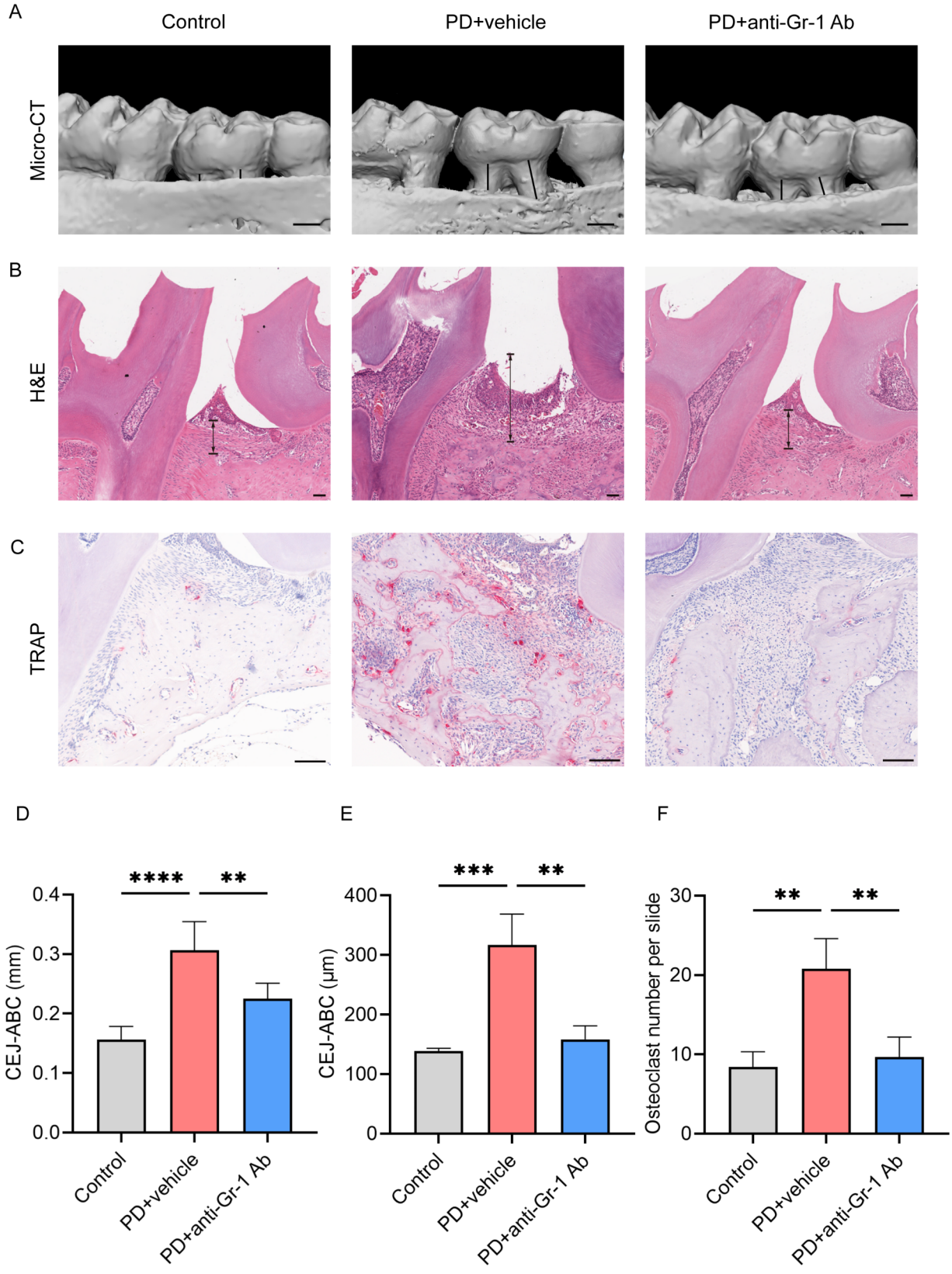


**Fig. 4** (See legend on next page.)

(See figure on previous page.)

**Fig. 4** MDSCs depletion alleviates periodontitis and reduces inflammation. (**A**) 3D reconstructions of maxillae from each group ($n = 5$ per group) were generated by micro-CT on day 28 after ligature removal. The vertical line extends from the CEJ to the ABC. The CEJ-ABC distance was measured at six predetermined sites on both the buccal and palatal sides. Scale bar = 50 μm. (**B**) Histological H&E staining of the periodontium in mice of each group. The vertical line extends from the CEJ to the ABC. The CEJ-ABC distance was quantified in each microscopic field of view. Scale bar = 50 μm. (**C**) Histological TRAP staining of the periodontium in mice of each group. Osteoclasts are stained red. The number of osteoclasts was quantified in each microscopic field of view. Scale bar = 100 μm. (**D**) Statistical analysis of the CEJ-ABC distance in each group ($n = 5$ per group) as analyzed by micro-CT. (**E**) Statistical analysis of the CEJ-ABC distance in each group ($n = 3$ per group) as analyzed by H&E staining. (**F**) Statistical analysis of the number of osteoclasts in each group ($n = 3$ per group) as determined by TRAP staining. Results are expressed as means ± S.D. $^{**}p < 0.01$; $^{****}p < 0.0001$ (one-way ANOVA with the correction of Bonferroni)

expression of NLRP3 in mouse macrophages and then activates the NLRP3 inflammasome to promote its assembly and subsequent processing by pro-caspase-1 [15]. Zhong et al. also confirmed that NF-κB facilitates the transcription of NLRP3 by binding to its promoter region, thereby increasing NLRP3 expression in the inflammatory response, which promotes the activation of the NLRP3 inflammasome [35]. Therefore, we speculate that Neat1 may promote the activation of NF-κB signaling in PD M-MDSCs, thereby activating the NLRP3 inflammasome, which ultimately leads to the massive production of the inflammatory factor IL-1β. We investigated the expression of NF-κB, NLRP3 inflammasome and relevant downstream molecules in PD mice. RT-qPCR analysis showed that the mRNA expression proinflammatory cytokines IL-1β, IL-6, and TNF-α was significantly increased in the periodontal tissues of the PD group compared with control group (Fig. 6A-C). These cytokines were reduced by 40%, 60%, and 50% in the PD + Gr-1 Ab group compared with those of the PD + vehicle group (Fig. 6A-C). Western blot analysis revealed a significant upregulation of pP65, NLRP3, cleaved caspase-1, and cleaved IL-1β at the protein level in PD. Conversely, depletion of MDSCs resulted in a significant downregulation of these proteins (Fig. 6D, E). Serum IL-1β, which can be secreted by inflamed tissues with NLRP3 and caspase-1 activation, contributes to the enhancement of the inflammatory response in PD. The ELISA results demonstrated that serum IL-1β levels were significantly decreased in the PD + Gr-1 Ab group compared to the PD + vehicle group (Fig. 6F). Moreover, the serum levels of other proinflammatory cytokines, IL-6 and TNF-α, were also reduced in the PD + Gr-1 Ab group (Fig. 6G, H). Collectively, the activation of the NF-κB-dependent "canonical NLRP3 inflammasome" pathway has been demonstrated in PD, offering valuable insight into the potential molecular mechanisms through which M-MDSCs contribute to the inflammatory progression of periodontitis.

## Discussion

In the present study, we investigated the role of M-MDSCs in periodontitis. Overall, we found that M-MDSCs significantly increased in gingiva of PD patients and mice. Depletion of M-MDSCs in PD mice could ameliorate alveolar bone loss and reduce periodontal tissue inflammation. Mechanistically, our results indicate that long non-coding RNA Neat1 is significantly upregulated in M-MDSCs, where it exerts its proinflammatory effect by activating NF-κB signaling in the context of PD. In addition, the activation of the NF-κB-dependent "canonical NLRP3 inflammasome" pathway was confirmed in a PD mouse model, leading to increased secretion of proinflammatory cytokines that drive alveolar bone loss, such as IL-1β, IL-6, and TNF-α (Fig. 7). To our knowledge, this is the first evidence indicating that the dysregulation of M-MDSCs contributes to the pathogenesis and progression of PD.

MDSCs are a heterogeneous cell group composed of morphologically, phenotypically, and functionally diverse but also highly immunosuppressive myeloid cells. They are generated and expanded under the pathological conditions of a tumor, inflammation, infection, etc [5]. While numerous studies have demonstrated the immunosuppressive role of MDSCs in various immune disorders, Chen et al. showed that M-MDSCs can program Th17 cells toward a pro-osteoclastogenic phenotype, which in turn potentiates osteoclast differentiation via the receptor activator of nuclear factor κB ligand (RANK-L)-RANK signaling [36]. Other studies have also identified a potentially significant proinflammatory role of MDSCs in rheumatoid arthritis and systemic lupus erythematosus [37, 38]. *Porphyromonas gingivalis* (*P. gingivalis*), the key bacterium in the pathogenesis of periodontitis, has been shown to stimulate the production of M-MDSCs in vitro in the presence of macrophage-colony stimulating factor (M-CSF) [39]. In animal models of *P. gingivalis*-induced periodontitis and rheumatoid arthritis, expansion of M-MDSCs in the blood and exacerbation of arthritis symptoms are observed [39]. In our study, we first isolated M-MDSCs in periodontal tissues using scRNA-seq analysis and found that M-MDSCs were increased in the gingiva of PD mice, suggesting that PD may enhance the local and systemic accumulation of M-MDSCs.

Interestingly, M-MDSCs tended to expand in the inflamed periodontium, whereas G-MDSCs did not. In autoimmune diseases, G-MDSCs exert suppressive effects, contributing to the inhibition of autoimmune responses, whereas M-MDSCs are primarily involved in promoting inflammatory responses, such as facilitating

Th17 cell differentiation, in experimental autoimmune encephalomyelitis and arthritis [40]. Indeed, M-MDSCs are notably present in tissues undergoing chronic inflammation, which partly explains the expansion of M-MDSCs in periodontitis. Furthermore, G-MDSCs are recruited primarily by CXC chemokines like CXCL1, CXCL2, and CXCL5, and the CCL2–CCR2 axis are crucial in directing the trafficking and recruitment of M-MDSCs to inflamed tissues [41]. Shen et al. demonstrated that Bindarit alleviated alveolar bone loss and reduced proinflammatory monocyte infiltration by inhibiting CCL2 in diabetes-associated periodontitis [42]. This suggests that M-MDSCs are likely recruited to inflamed gingival tissues via CCL2. However, the specific role of the chemokines in MDSCs trafficking warrants further investigation.

Furthermore, we utilized an anti-mouse Gr1 Ab to deplete MDSCs in our study. Recent studies of ligature-induced PD in mice have shown that therapeutic intervention can be performed during the initiation (simultaneous with ligature placement), progression (several days after ligature placement), or resolution (after ligature removal) phases [43, 44]. Kourtzelis et al. [44] and Shehabeldin, et al. [43] have reported that, following the removal of ligatures in mice with ligature-induced periodontitis, there is a slow spontaneous healing of the periodontium and a cessation of progressive bone loss. To clarify the role of MDSCs in PD in vivo, we depleted MDSCs in mice with ligature-induced periodontitis after ligatures removal. In our study, we investigated the pro-healing effect with removal of ligatures by the delivery of anti-mouse Gr-1 Ab [42, 45]. Our results confirmed that depletion of MDSCs in mice with ligature-induced periodontitis after ligature removal led to a reduction in inflammatory cell infiltration, a decrease in osteoclast numbers, and an acceleration of bone regeneration compared to mice with ligature-induced periodontitis alone. In arthritis, Zhang et al. have shown that depletion of MDSCs by Gr-1 Ab inhibits the inflammatory response in mice with collagen-induced arthritis and induces the Th17 response [46]. Another study also observed that depletion of M-MDSCs reduced the number of osteoclasts, cartilage damage and immune infiltration, which is consistent with the results of our study [36].

As key regulators of immune responses, lncRNAs are involved in the production of inflammatory mediators, cell differentiation and migration. Neat1 is a ubiquitously expressed lncRNA that is enriched in the nucleus for paraspeckle formation [34]. Recent studies have shown that Neat1 plays a critical role in promoting antigen-specific Th17 cell responses in uveitis and other Th17 cell-mediated autoimmune diseases [47]. Dong et al. also have found that Neat1, but not its isoform Neat1_2, is upregulated in G-MDSCs during lupus progression [48]. Here, we identified that the expression of Neat1, including Neat1_1 and Neat1_2, was significantly elevated in M-MDSCs of PD in scRNA-seq data and in ligature-induced periodontitis mice, suggesting the upregulation of Neat1 in PD. Previous studies also showed that Neat1 was highly expressed in PD tissues or periodontal ligament stem cells (PDLSCs) with nicotine treatment [49]. In addition, knockdown of Neat1 significantly attenuated both the inflammatory response and apoptosis in LPS-induced PDLCs [13]. In the present study, Neat1 expression was found to be reduced upon the depletion of MDSCs in ligature-induced periodontitis mice, indicating that Neat1 is highly expressed in MDSCs and plays a potential role in promoting inflammation in periodontal disease through MDSCs.

Neat1 has been identified as an upstream target of NF-κB signaling, a major receptor-mediated pathway induced by LPS [50]. This signaling pathway plays a crucial role in the immune response by regulating the transcription of inflammatory genes, including NLRP3 [51]. In titanium particle-induced osteolysis, Neat1 exacerbates the inflammatory response by activating the NF-κB pathway, which subsequently induces NLRP3 inflammation formation and promotes M1 macrophage polarization [32]. Macrophages infected with *P. gingivalis* can also activate NF-κB, resulting in the formation of pro-IL-1β and upregulated NLRP3 expression [52]. Similarly, our scRNA-seq analysis revealed activation of the TNF-α/NF-κB signaling pathway in M-MDSCs in periodontal disease. We also demonstrated that the NF-κB pathway is active in PD mice and that its activation is suppressed following MDSCs depletion, suggesting a potential dysregulation of NF-κB signaling in this context. Furthermore, we found that NLRP3, a key inflammatory molecule downstream of NF-κB, was transcriptionally upregulated, resulting in the activation of the NLRP3 inflammasome. This activation subsequently led to an elevated production of the proinflammatory cytokines IL-1β, IL-6, and TNF-α. These findings suggest a potential relationship among Neat1, NF-κB, and NLRP3, which is consistent with previous studies [15, 32]. However, our study does not address the relationship among Neat1, NF-κB, and NLRP3 in M-MDSCs in PD through loss- and gain-of-function approaches. Future research is needed to elucidate the mechanism by which Neat1 regulates NF-κB and NLRP3 transcription in periodontitis, particularly using Neat1-deficient mouse models.

The NLRP3 inflammasome, composed of NLRP3, apoptosis-associated speck-like protein containing a caspase-1 recruitment domain (ASC) and pro-caspase-1, is associated with the pathogenesis of periodontal disease. Upon activation, the NLRP3 inflammasome triggers caspase-1 activation, which facilitates the maturation of IL-1β and IL-18 [53]. The release of these proinflammatory

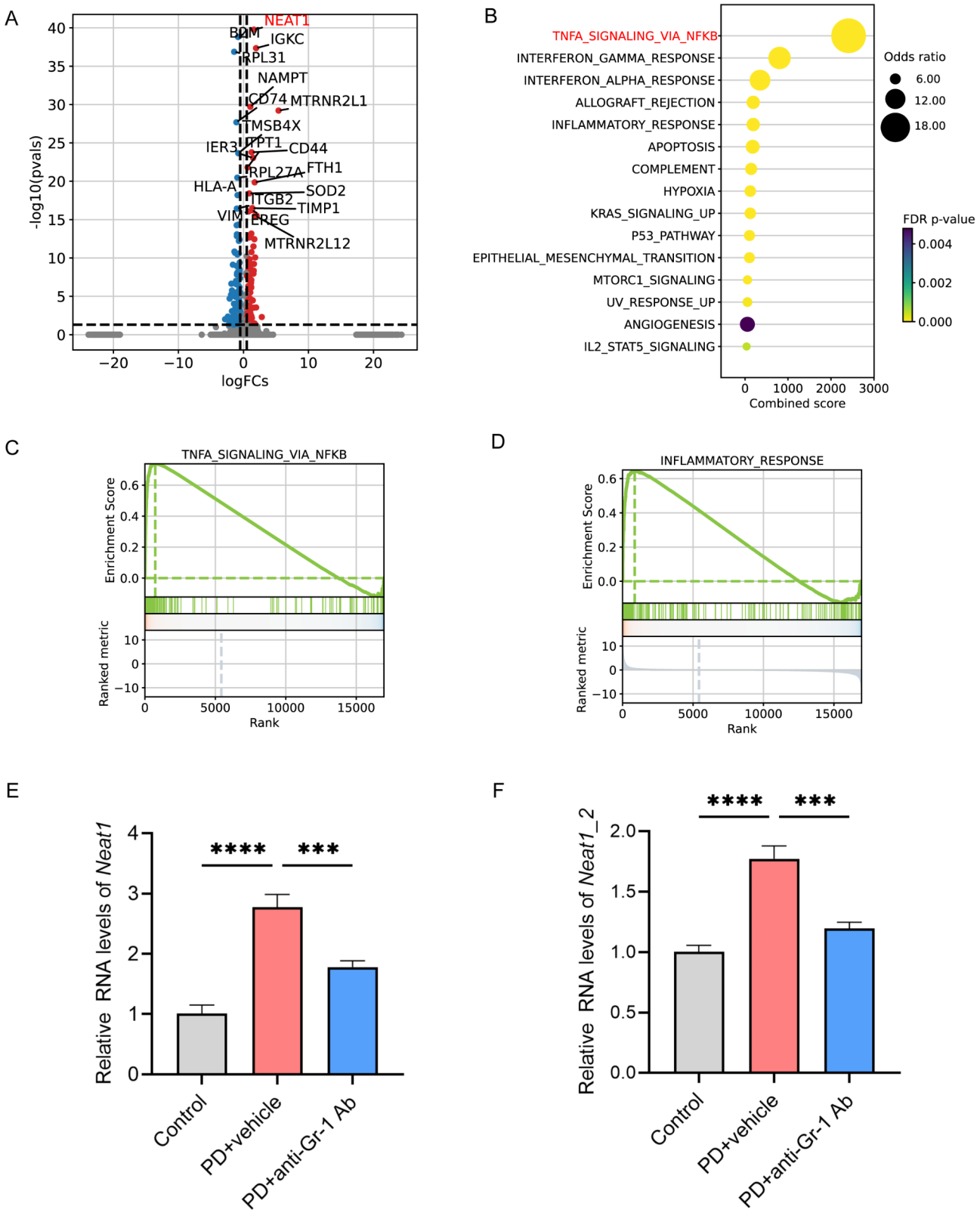


**Fig. 5** Neat1 expression is upregulated in PD. (**A**) Volcano plots showing DEGs of M-MDSCs between PD and HC in scRNA-seq data. (**B**) GO functional analysis of the DEGs with significance below 0.05 in M-MDSCs between PD and HC. (**C**-**D**) GSEA showing the DEGs distribution of TNFA signaling via NF-κB pathway (**C**) and inflammatory response pathway (**D**). (**E**) The mRNA expression levels of Neat1 and Neat1_2 in the periodontium of each group ($n = 3$ per group) were analyzed by RT-qPCR on day 28 after ligature removal. Results are presented as means ± S.D. $^{**}p < 0.01$; $^{****}p < 0.0001$ (one-way ANOVA with the correction of Bonferroni)

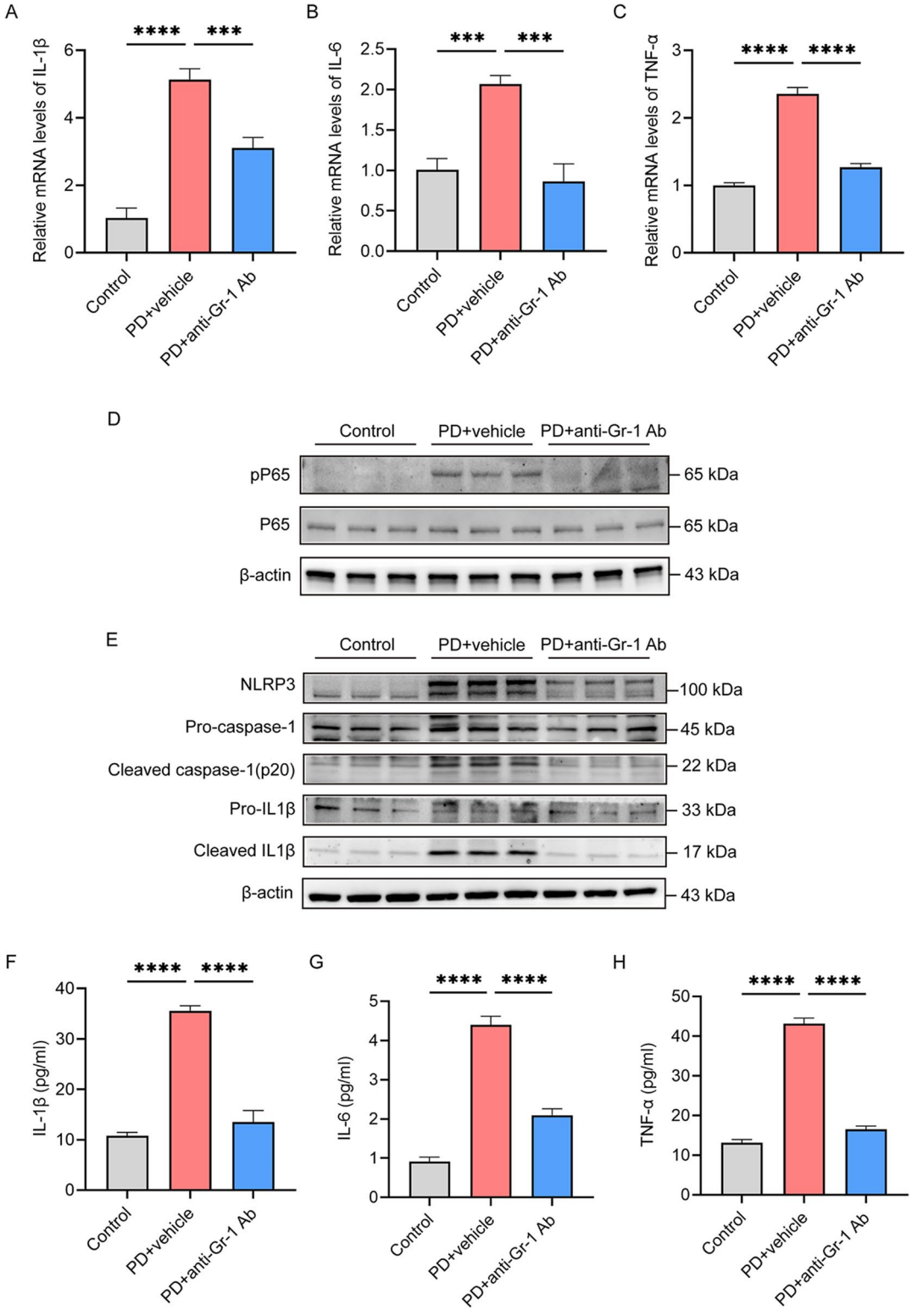


**Fig. 6** MDSCs depletion reduces the activation of NF-κB signaling and NLRP3 inflammasome in PD. (**A**-**C**) The mRNA expression levels of IL1-β, IL-6, and TNF-α in periodontal tissues of each group ($n = 3$ per group) were analyzed by RT-qPCR. (**D**) P65 and pP65 levels in the periodontal tissues of each group were measured by Western blot analysis ($n = 3$ per group) (**E**) NLRP3, pro-caspase-1, cleaved caspase-1, pro-IL-1β, and cleaved IL-1β levels in the periodontal tissues of each group were measured by Western blot analysis ($n = 3$ per group). (**F**-**H**) IL-1β, IL-6, and TNF-α protein levels in the gingiva of each group ($n = 3$ per group) were analyzed by ELISA. The results were presented as means ± S.D. *$p < 0.05$; **$p < 0.01$; ***$p < 0.001$; ****$p < 0.0001$(one-way ANOVA with the correction of Bonferroni)

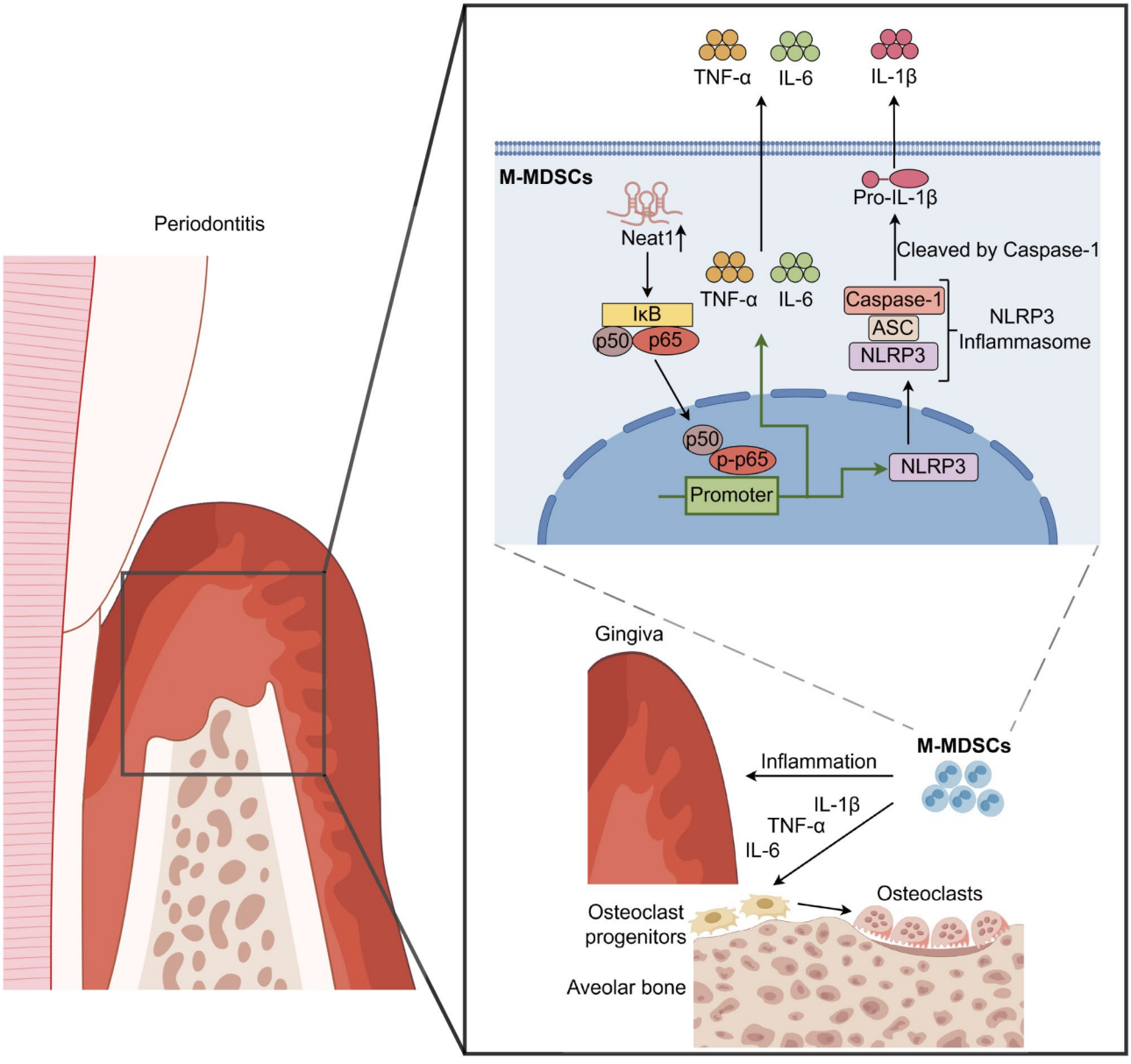


**Fig. 7** A model depicting how M-MDSCs regulate alveolar bone loss in ligature-induced periodontitis. M-MDSCs expansion in periodontitis promotes inflammation and drives alveolar bone loss via upregulating Neat1, where it exerts its proinflammatory effect by activating NF-κB signaling. Subsequently, the NF-κB-dependent "canonical NLRP3 inflammasome" pathway is activated, leading to increased secretion of proinflammatory cytokines, such as IL-1β, IL-6, and TNF-α

cytokines could promote the activation and recruitment of various immune cells, including macrophages, neutrophils, and MDSCs to sites of infection or injury [54]. In ligature-induced periodontitis or aged-related periodontitis, inhibition of the NLRP3 inflammasome by NLRP3 inhibitor MCC950 suppresses osteoclastic differentiation and promotes healing of alveolar bone defects [55]. Consequently, we investigated the expression profiles of NLRP3 and IL-1β. We demonstrated that NLRP3 inflammasome was activated and IL-1β, along with other proinflammatory cytokines such as IL-6 and TNF-α, was upregulated in PD.

Recently, there has been a growing interest among researchers in targeted immunotherapy approaches for the treatment of chronic inflammatory diseases, including cancer and autoimmune disorders, etc. Investigations have focused on therapies targeting MDSCs to mitigate tumor evasion in cancer. For instance, a phase I clinical trial demonstrated that the agonist antibody DS-8273a, which targets the TRAIL receptor 2, can rapidly and selectively eliminate MDSCs in cancer patients [56]. In

lupus nephritis patients, treatment with rituximab or obinutuzumab, which target the CD20 antigen on B cells, have effectively decreased proteinuria and improved renal function [57, 58]. Interestingly, recent studies demonstrated that local delivery of the chemokine CCL2 or the cytokine IL-4 in murine ligature-induced periodontitis effectively reduced inflammatory bone loss during disease progression and facilitated bone regeneration during disease resolution, specifically targeting macrophages [43, 59]. Our study also showed a favorable therapeutic effect with depletion of MDSCs in mouse models of PD, as evidenced by a reduction in inflammation and downregulation of inflammatory factors. This suggests that targeting immune cells of myeloid origin is a promising direction for future research in chronic inflammatory diseases such as periodontitis.

This study presents several limitations that need to be acknowledged. Firstly, the sample size used in our experiments was relatively small, which may limit the generalizability of our findings to broader populations. In addition, the research was conducted within a single experimental model, which limits the ecological validity of the results. The absence of longitudinal clinical data further limits our ability to examine the long-term effects of M-MDSCs activity in periodontitis. These limitations underscore the necessity for further investigation using larger, more diverse cohorts and multiple experimental approaches to validate the role of M-MDSCs and related molecular pathways in periodontitis.

In conclusion, our study highlights the potential proinflammatory role of M-MDSCs in both human and animal models of periodontitis. Based on these observations, it can be inferred that targeting M-MDSCs may offer a promising and innovative therapeutic strategy for managing periodontitis. Future research could investigate strategies aimed at specifically targeting M-MDSCs for the treatment of periodontitis.

## Supplementary Information

The online version contains supplementary material available at https://doi.org/10.1186/s12967-025-06214-x .

Supplementary Material 1

**Acknowledgements**
There are no acknowledgments to declare.

**Author contributions**
Zhaocai Zhou, Zhengmei Lin, and Zhi Song conceived the study and designed experiments. Zhaocai Zhou, Chi Zhan, and Wenchuan Li performed the majority of the experiments, interpreted the data and wrote the manuscript. Wenji Luo contributed to in vivo experiments. Yufeng Liu and Feng He contributed to revising manuscript content. Yaguang Tian, Zhengmei Lin, and Zhi Song supervised the entire project and approved the final version of manuscript. All authors approved the final version of the manuscript. All authors listed have made a substantial, direct, and intellectual contribution to the work and approved it for publication.

**Funding**
This study was supported by grants from the National Natural Science Foundation of China (Grant No. 82470748, 81860195, and 82170939), Guangdong Natural Science Foundation (Grant No. 2023A1515010519), Hainan Provincial Natural Science Foundation of China (No. 822CXTD534), and Hainan Province Science and Technology Special Fund (No. ZDYF2021SHFZ229).

**Data availability**
The datasets supporting the conclusions of this article are included within the article and its additional file. For any further data requests, please contact the corresponding authors.

## Declarations

**Ethics approval and consent to participate**
The animal study protocol was approved by the Ethics Committee of the Animal Care and Use Committee of Sun Yat-sen University (No. 2024001340). The human subject protocol was approved by the Medical Ethics Committee of Hospital of Stomatology, Sun Yat-sen University (KQEC-2022-06), and all participants had informed consent.

**Consent for publication**
All authors have reviewed the final version of the manuscript and approved it for publication.

**Competing interests**
The authors declare that they have no competing interests.

**Author details**
[1]Hospital of Stomatology, Guangdong Provincial Key Laboratory of Stomatology, Guanghua School of Stomatology, Sun Yat-sen University, Guangzhou 510055, China
[2]Guangzhou First People's Hospital, The Second Affiliated Hospital, School of Medicine, South China University of Technology, Guangzhou 510180, China
[3]Department of Stomatology, Hainan General Hospital, Hainan Affiliated Hospital of Hainan Medical University, Haikou 570311, China

Received: 20 November 2024 / Accepted: 7 February 2025
Published online: 21 February 2025

**References**

1. Nascimento PC, Castro MML, Magno MB, et al. Association between periodontitis and cognitive impairment in adults: a systematic review. Front Neurol. 2019;10:323.
2. Genco RJ, Sanz M. Clinical and public health implications of periodontal and systemic diseases: an overview. Periodontol 2000. 2020;83:7–13.
3. Balta MG, Papathanasiou E, Blix IJ, et al. Host modulation and treatment of periodontal disease. J Dent Res. 2021;100:798–809.
4. Luan J, Li R, Xu W, et al. Functional biomaterials for comprehensive periodontitis therapy. Acta Pharm Sin B. 2023;13:2310–33.
5. Gabrilovich DI, Nagaraj S. Myeloid-derived suppressor cells as regulators of the immune system. Nat Rev Immunol. 2009;9:162–74.
6. Peranzoni E, Zilio S, Marigo I, et al. Myeloid-derived suppressor cell heterogeneity and subset definition. Curr Opin Immunol. 2010;22:238–44.
7. Bronte V, Brandau S, Chen SH, et al. Recommendations for myeloid-derived suppressor cell nomenclature and characterization standards. Nat Commun. 2016;7:12150.
8. Ma T, Renz BW, Ilmer M et al. Myeloid-derived suppressor cells in solid tumors. Cells. 2022;11.
9. Cheng R, Billet S, Liu C, et al. Periodontal inflammation recruits distant metastatic breast cancer cells by increasing myeloid-derived suppressor cells. Oncogene. 2020;39:1543–56.
10. Kwack KH, Zhang L, Sohn J, et al. Novel preosteoclast populations in obesity-associated periodontal disease. J Dent Res. 2022;101:348–56.
11. Chen YG, Satpathy AT, Chang HY. Gene regulation in the immune system by long noncoding rnas. Nat Immunol. 2017;18:962–72.

12. Liu R, Tang A, Wang X, et al. Inhibition of lncrna neat1 suppresses the inflammatory response in ibd by modulating the intestinal epithelial barrier and by exosome-mediated polarization of macrophages. Int J Mol Med. 2018;42:2903–13.
13. Zhang L, Lv H, Cui Y, et al. The role of long non-coding rna (lncrna) nuclear paraspeckle assembly transcript 1 (neat1) in chronic periodontitis progression. Bioengineered. 2022;13:2336–45.
14. Murakami T, Nakaminami Y, Takahata Y et al. Activation and function of nlrp3 inflammasome in bone and joint-related diseases. Int J Mol Sci. 2022;23.
15. Zhang P, Cao L, Zhou R, et al. The lncrna neat1 promotes activation of inflammasomes in macrophages. Nat Commun. 2019;10:1495.
16. Williams DW, Greenwell-Wild T, Brenchley L, et al. Human oral mucosa cell atlas reveals a stromal-neutrophil axis regulating tissue immunity. Cell. 2021;184:4090–e41044015.
17. Chen Y, Wang H, Yang Q, et al. Single-cell rna landscape of the osteoimmunology microenvironment in periodontitis. Theranostics. 2022;12:1074–96.
18. Wolf FA, Angerer P, Theis FJ, Scanpy. Large-scale single-cell gene expression data analysis. Genome Biol. 2018;19:15.
19. Lopez R, Regier J, Cole MB, et al. Deep generative modeling for single-cell transcriptomics. Nat Methods. 2018;15:1053–8.
20. Bernstein NJ, Fong NL, Lam I, et al. Solo: doublet identification in single-cell rna-seq via semi-supervised deep learning. Cell Syst. 2020;11:95–e101105.
21. Zhang L, Li Z, Skrzypczynska KM, et al. Single-cell analyses inform mechanisms of myeloid-targeted therapies in colon cancer. Cell. 2020;181:442–e459429.
22. Alshetaiwi H, Pervolarakis N, McIntyre LL et al. Defining the emergence of myeloid-derived suppressor cells in breast cancer using single-cell transcriptomics. Sci Immunol. 2020;5.
23. Badia IMP, Vélez Santiago J, Braunger J, et al. Decoupler: ensemble of computational methods to infer biological activities from omics data. Bioinform Adv. 2022;2:vbac016.
24. Marchesan J, Girnary MS, Jing L, et al. An experimental murine model to study periodontitis. Nat Protoc. 2018;13:2247–67.
25. Cai B, Liu Y, Chong Y, et al. Irak1-regulated ifn-γ signaling induces mdsc to facilitate immune evasion in fgfr1-driven hematological malignancies. Mol Cancer. 2021;20:165.
26. Zhang Y, Chen J, Fu H, et al. Exosomes derived from 3d-cultured mscs improve therapeutic effects in periodontitis and experimental colitis and restore the th17 cell/treg balance in inflamed periodontium. Int J Oral Sci. 2021;13:43.
27. Sawant A, Ponnazhagan S. Myeloid-derived suppressor cells as osteoclast progenitors: a novel target for controlling osteolytic bone metastasis. Cancer Res. 2013;73:4606–10.
28. Zhong L, Li S, Wen Y, et al. Expansion of polymorphonuclear myeloid-derived suppressor cells in patients with gout. Front Immunol. 2020;11:567783.
29. Zhang H, Huang Y, Wang S, et al. Myeloid-derived suppressor cells contribute to bone erosion in collagen-induced arthritis by differentiating to osteoclasts. J Autoimmun. 2015;65:82–9.
30. Ouzounova M, Lee E, Piranlioglu R, et al. Monocytic and granulocytic myeloid derived suppressor cells differentially regulate spatiotemporal tumour plasticity during metastatic cascade. Nat Commun. 2017;8:14979.
31. Kinane DF, Stathopoulou PG, Papapanou PN. Periodontal diseases. Nat Rev Dis Primers. 2017;3:17038.
32. Lin S, Wen Z, Li S, et al. Lncrna neat1 promotes the macrophage inflammatory response and acts as a therapeutic target in titanium particle-induced osteolysis. Acta Biomater. 2022;142:345–60.
33. Ma J, Zhao N, Du L, et al. Downregulation of lncrna neat1 inhibits mouse mesangial cell proliferation, fibrosis, and inflammation but promotes apoptosis in diabetic nephropathy. Int J Clin Exp Pathol. 2019;12:1174–83.
34. Fox AH, Nakagawa S, Hirose T, et al. Paraspeckles: where long noncoding rna meets phase separation. Trends Biochem Sci. 2018;43:124–35.
35. Zhong Z, Umemura A, Sanchez-Lopez E, et al. Nf-κb restricts inflammasome activation via elimination of damaged mitochondria. Cell. 2016;164:896–910.
36. Chen S, Guo C, Wang R, et al. Monocytic mdscs skew th17 cells toward a pro-osteoclastogenic phenotype and potentiate bone erosion in rheumatoid arthritis. Rheumatology (Oxford). 2021;60:2409–20.
37. Wu H, Zhen Y, Ma Z, et al. Arginase-1-dependent promotion of th17 differentiation and disease progression by mdscs in systemic lupus erythematosus. Sci Transl Med. 2016;8:331ra340.
38. Guo C, Hu F, Yi H, et al. Myeloid-derived suppressor cells have a proinflammatory role in the pathogenesis of autoimmune arthritis. Ann Rheum Dis. 2016;75:278–85.
39. Zhou N, Zou F, Cheng X, et al. Porphyromonas gingivalis induces periodontitis, causes immune imbalance, and promotes rheumatoid arthritis. J Leukoc Biol. 2021;110:461–73.
40. Rui K, Peng N, Xiao F, et al. New insights into the functions of mdscs in autoimmune pathogenesis. Cell Mol Immunol. 2023;20:548–50.
41. Lasser SA, Ozbay Kurt FG, Arkhypov I, et al. Myeloid-derived suppressor cells in cancer and cancer therapy. Nat Rev Clin Oncol. 2024;21:147–64.
42. Shen Z, Kuang S, Zhang M, et al. Inhibition of ccl2 by bindarit alleviates diabetes-associated periodontitis by suppressing inflammatory monocyte infiltration and altering macrophage properties. Cell Mol Immunol. 2021;18:2224–35.
43. Shehabeldin M, Gao J, Cho Y, et al. Therapeutic delivery of ccl2 modulates immune response and restores host-microbe homeostasis. Proc Natl Acad Sci U S A. 2024;121:e2400528121.
44. Kourtzelis I, Li X, Mitroulis I, et al. Del-1 promotes macrophage efferocytosis and clearance of inflammation. Nat Immunol. 2019;20:40–9.
45. Wang Y, Chu T, Jin T, et al. Cascade reactions catalyzed by gold hybrid nanoparticles generate co gas against periodontitis in diabetes. Adv Sci (Weinh). 2024;11:e2308587.
46. Zhang H, Wang S, Huang Y, et al. Myeloid-derived suppressor cells are proinflammatory and regulate collagen-induced arthritis through manipulating th17 cell differentiation. Clin Immunol. 2015;157:175–86.
47. Chen S, Wang J, Zhang K, et al. Lncrna neat1 targets nono and mir-128-3p to promote antigen-specific th17 cell responses and autoimmune inflammation. Cell Death Dis. 2023;14:610.
48. Dong G, Yang Y, Li X, et al. Granulocytic myeloid-derived suppressor cells contribute to ifn-i signaling activation of b cells and disease progression through the lncrna neat1-baff axis in systemic lupus erythematosus. Biochim Biophys Acta Mol Basis Dis. 2020;1866:165554.
49. Zhang T, Yang K, Chen Y, et al. Impaired autophagy flux by lncrna neat1 is critical for inflammation factors production in human periodontal ligament stem cells with nicotine treatment. J Periodontal Res. 2023;58:70–82.
50. Bai YH, Lv Y, Wang WQ, et al. Lncrna neat1 promotes inflammatory response and induces corneal neovascularization. J Mol Endocrinol. 2018;61:231–9.
51. Liu T, Zhang L, Joo D, et al. Nf-κb signaling in inflammation. Signal Transduct Target Ther. 2017;2:17023.
52. Huang MT, Taxman DJ, Holley-Guthrie EA, et al. Critical role of apoptotic speck protein containing a caspase recruitment domain (asc) and nlrp3 in causing necrosis and asc speck formation induced by porphyromonas gingivalis in human cells. J Immunol. 2009;182:2395–404.
53. Wang L, Hauenstein AV. The nlrp3 inflammasome: mechanism of action, role in disease and therapies. Mol Aspects Med. 2020;76:100889.
54. Dinarello CA. Interleukin-1 in the pathogenesis and treatment of inflammatory diseases. Blood. 2011;117:3720–32.
55. Chen Y, Yang Q, Lv C, et al. Nlrp3 regulates alveolar bone loss in ligature-induced periodontitis by promoting osteoclastic differentiation. Cell Prolif. 2021;54:e12973.
56. Dominguez GA, Condamine T, Mony S, et al. Selective targeting of myeloid-derived suppressor cells in cancer patients using ds-8273a, an agonistic trail-r2 antibody. Clin Cancer Res. 2017;23:2942–50.
57. Fanouriakis A, Kostopoulou M, Andersen J, et al. Eular recommendations for the management of systemic lupus erythematosus: 2023 update. Ann Rheum Dis. 2024;83:15–29.
58. Furie RA, Aroca G, Cascino MD, et al. B-cell depletion with obinutuzumab for the treatment of proliferative lupus nephritis: a randomised, double-blind, placebo-controlled trial. Ann Rheum Dis. 2022;81:100–7.
59. Shehabeldin M, Kobyra J, Cho Y, et al. Local controlled delivery of il-4 decreases inflammatory bone loss in a murine model of periodontal disease. J Immunol. 2024;213:1635–43.


## Publisher's note